ELSEVIER

Journal of Power Sources 113 (2003) 301–307

JOURNAL OF POWER SOURCES

www.elsevier.com/locate/jpowsour

Electrochemical study in sulphuric acid of the hardening $L1_2$ phases of Pb–Ca–Sn alloys

G. Bourguignon[a], A. Maître[a,*], E. Rocca[a], J. Steinmetz[a], L. Torcheux[b]

[a]*Laboratoire de Chimie du Solide Minéral, UMR CNRS 7555, Universite Henri Poincare, bd des Aiguillettes BP 239, Vandoeuvre les Nancy Cedex F-54506, France*

[b]*CEAC, 5-7, allée des Pierres Mayettes, Gennevilliers F-92636, France*

Abstract

A study of the metallurgical transformations and of the electrochemical behaviour of Pb–0.08% Ca–*x*% Sn alloys has been performed. The corrosion resistance of five hardening $L1_2$ phases (Pb_3Ca, Pb_2SnCa, $Pb_{1.5}Sn_{1.5}Ca$, $PbSn_2Ca$, Sn_3Ca) has been characterised. It is found that high tin contents in alloys improve the mechanical properties and their corrosion resistance in sulphuric acid. Furthermore, the most favourable metallurgical state, i.e. the ''aged'' state appears stabilised by a tin content of around 2 wt.%. In the same manner, the rate of corrosion in overcharge conditions dramatically increases for Pb–Ca–Sn overaged alloys. These results seem to be linked to the tin level in the matrix, although the corrosion resistance of the $L1_2$ phases rises with the tin content.

Keywords: Ageing; Overageing; Pb–Ca–Sn alloys; Electrochemical corrosion; Mechanical properties; $L1_2$ intermetallics

1. Introduction

During the past 10 years, most manufacturers of lead-acid batteries have opted for lead–calcium–tin base alloys as the materials of choice for the positive grids in applications such as the starting–lighting–ignition of vehicles, standby power, or storage in photovoltaic systems. Compared to the lead–antimony alloys, the lead–calcium alloys do not suffer significant water loss in service but require tin addition to improve their corrosion resistance in overcharge conditions and to avoid the passivation phenomenon in conditions of deep discharge [1–3]. Moreover, tin influences the mechanical properties of the alloys. In binary lead–calcium alloys, the hardness increases after casting leads to the aged state, which is due to the precipitation of an intermetallic phase, Pb_3Ca, of $L1_2$-type structure (space group: $Pm3m$). Additions of tin modify the ageing conditions. According to Prengaman [4], Sn_3Ca is a more stable strengthening compound than Pb_3Ca and, in order to provide stable precipitates of Sn_3Ca, at least a 9:1 Sn/Ca weight ratio is required. For lower ratios, for example around 7 [5], a Pb–Ca–Sn alloy exhibits four transformations namely:

- a linear, discontinuous, transformation immediately after cooling;
- a second transformation with an irregular motion of grain boundaries, called ''puzzling'', generally achieved after 24 h;
- a continuous and fine precipitation of $Pb_{3-x}Sn_xCa$ phase, isostructural with Pb_3Ca, leading to the ageing;
- finally, a discontinuous transformation related to the reaction:

$$Pb_{3-x}Sn_xCa_{\text{fine dispersed precipitates}} \rightarrow Pb_{3-x}Sn_xCa_{\text{large lamellar precipitates}},\ \text{called overaging.}$$

Overageing is consecutive to the coalescence of the precipitates, driven by the need to minimise the surface energy as well as by the chemical oversaturation of the lead matrix. At the same time, overageing provokes a decrease in the corrosion resistance, mainly during the overcharge periods of the battery, and a drop in the mechanical properties, observed through the hardness decrease. Consequently, for applications such as those concerning photovoltaic energy storage or the electric vehicle, the grids can undergo

* Corresponding author. Tel.: +33-383-68-4656; fax: +33-383-68-4611.
E-mail address: alexandre.maitre@lcsm.uhp-nancy.fr (A. Maître).

0378-7753/02/$ – see front matter
PII: S0378-7753(02)00525-6

an accelerated corrosion phase during the boost charge or the recharge periods. As the overaged state is more delayed as the tin content rises, the overall objective of the present study was to determine more accurately the relationship between microstructure and corrosion behaviour. This project required analysis of the hardening precipitate composition, using transmission electron microscopy coupled with energy dispersive X-ray spectrometry, and knowledge of their intrinsic corrosion behaviour, mainly in conditions of overvoltage in H_2SO_4.

2. Experimental

2.1. Materials

2.1.1. Synthesis of alloys

Specimens of Pb–Ca–Sn alloys were synthesised from a Pb–0.12 wt.% Ca master alloy furnished by Compagnie Européenne d'Accumulateurs (CEAc, France), pure lead (99.95%, GoodFellow) and pure tin (99.99%, Prolabo). The raw materials were melted at 923 K for about an hour, then cast in an iced copper mould. The compositions of the ternary alloys so obtained are given in Table 1. Finally the different alloys were made in the shape of plates (60 mm × 60 mm × 3 mm).

2.1.2. Synthesis of intermetallics

Five pure phases belonging to the $Pb_{3-x}Sn_xCa$ solid solution have been synthesised. Their formulae are Pb_3Ca, Pb_2SnCa, $Pb_{1.5}Sn_{1.5}Ca$, $PbSn_2Ca$, and Sn_3Ca. Considering the high reactivity of calcium vis-à-vis the oxygen, these phases were elaborated with care. Indeed, Pb_3Ca, Pb_2SnCa and $Pb_{1.5}Sn_{1.5}Ca$ were prepared from elements of high purity in an induction furnace, under argon atmosphere, after having been pressed in a glove box. $PbSn_2Ca$ and Sn_3Ca were elaborated differently: pellets of pressed elements were introduced into a molybdenum tube, itself capped by an alumina tube, the two tubes being maintained in a quartz vessel. Once a pressure close to 10^{-6} bar was reached, the vessel was sealed, then heated to 1473 K, before being turned over, in order to facilitate the liquid transfer towards the alumina tube. A last annealing at 723 K improves the alloy homogenisation. The chemical composition of the intermetallic phases was determined by EPMA (Cameca SX50) and by X-ray diffraction (Philips X'Pert Pro).

Table 1
Chemical analysis using atomic absorption spectrometry and electronic microprobe analysis, of the lead–calcium–tin alloys

Alloy	Ca (wt.%)[a]	Sn (wt.%)[b]
Pb–0.08% Ca	0.074	0.02
Pb–0.08% Ca–0.6% Sn	0.073	0.58
Pb–0.08% Ca–1.2% Sn	0.076	1.11
Pb–0.08% Ca–2.0% Sn	0.075	1.96

[a] Using atomic absorption spectrometry.
[b] Using electronic microprobe analysis.

2.2. Characterisation

2.2.1. TEM study

Thin foils for TEM studies were prepared by different methods in accordance with their metallurgical state as described in a previous article [6]:

- for overaged alloys, the required procedure consists of: (i) preparation of a small block (4 mm × 3 mm × 12 mm) from the plate core; (ii) cutting of thin foils (≤100 nm) from this block by ultramicrotomy (Ultramicrotome Reichert Ultracute);
- for aged alloys, since their transformation into the overaged state is favoured by strain hardening, it was preferable to prepare thin foils using microtomy (≤5 μm) then argon-ion milling.

These foils were examined in a Philips-CM20 electron microscope operating at 200 kV. This instrument is equipped with an energy dispersive X-ray spectrometer (EDXS), allowing chemical analysis of the precipitates.

2.2.2. Hardness measurements

Vickers hardness measurements (under a loading charge of 20 N) were carried out for each sample using a macro-Vickers hardness tester (Testwell-type). The hardness data were determined from the average of at least five hardness readings from each sample. The average hardness data were found to be reproducible within 5%.

2.2.3. Electrochemical tests

For the specimens of Pb–Ca–Sn alloys, electrochemical tests were performed in a three-electrode electrochemical cell, which was connected to a radiometer or a EGG Princeton potentiostat and driven by a computer. The circular and horizontal working electrode ($S = 2.7$ cm^2) was placed at the bottom under a Pt-disk electrode. The electrolyte was a 5 M sulphuric acid solution. The working electrode was mechanically polished with different grades of SiC papers as follows: 240, 400, 800, 1200 then with colloidal silica dispersed in water.

For the intermetallics a "submarine" electrochemical cell was used. The working electrode was immersed vertically opposite to the Pt-disk electrode.

For both apparatuses, the reference electrode was a K_2SO_4—saturated mercurous sulphate electrode ($E =$ 0.658 V/SHE). The working electrode potentials are always given with respect to this reference electrode.

Two experimental sequences were used according to the sample studied:

- For Pb–Ca–Sn samples, the weight loss was determined after a polarisation test at 1.5 V for 5 days at 323 K in 5 M concentrated sulphuric acid solution.

- For the intermetallic phases, the corrosion potential was followed for 4 h. The $i = f(E)$ potentiodynamic curve, from −2000 to 1700 mV was obtained with a sweep rate of 1 mV/s. Then electrochemical behaviour in conditions simulating battery overcharge was determined from a polarisation test at 1.5 V during 24 h at room temperature in 0.5 M sulphuric acid solution. Finally, the Pb/intermetallic couples were tested at room temperature in 0.5 M sulphuric acid solution.

The composition of the corrosion products was analysed by EPMA. SEM (Hitachi S-2500) observations were carried out to provide more information on the morphology of the corrosion layer.

3. Results

3.1. Microstructural study

3.1.1. Mechanical behaviour

Fig. 1 shows the hardness versus time for the Pb–0.08% Ca–(0, 0.6, 2.0 wt.%) Sn supersaturated alloys at 313 K, which is generally admitted as the working temperature of the lead-acid battery. At this temperature, it can be seen that the tin content has a significant influence on the alloy's mechanical behaviour. The quenched alloys present a low initial hardness similar to that of pure lead (6 H_v). Then, the hardness regularly increases up to a peak value that depends on the tin alloy content. Indeed, the hardness of the Pb–0.08% Ca–2.0% Sn alloy abruptly increases then reaches a value around 21 H_v as opposed to the 18 or 12 H_v obtained for Pb–0.08% Ca–0.6% Sn alloy and Pb–0.08% Ca alloy, respectively. Otherwise, it can be noted that overageing, which is accompanied by a rapid hardness drop, appears beyond the first days at 313 K for a lower alloy tin content (i.e. 0.6 wt.%). Conversely, the mechanical behaviour of a Pb–0.08% Ca–2.0% Sn alloy is not affected by the softening.

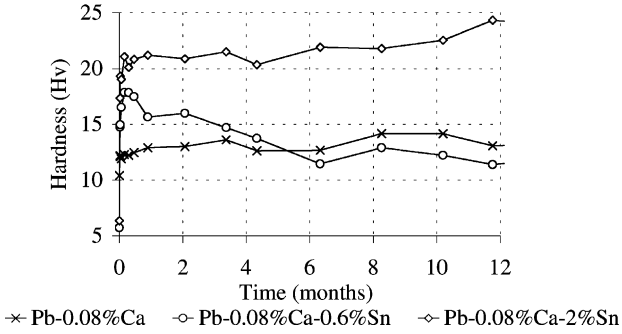

Fig. 1. Hardness evolution of Pb–0.08% Ca–x% Sn (with $x = 0$, 0.6 and 2%) alloys at 313 K.

3.1.2. Microstructural characterisation by TEM

This work complements the main results that have already been obtained during a first metallurgical study of the Pb–Ca–Sn alloys [6]. In particular, a more extensive study of precipitate composition in the course of the overageing process has been performed.

The two representative metallurgical states (aged and overaged) of Pb–Ca–Sn alloys have been isolated by appropriate thermal treatments based on analysis of TTT curves [7,8]: the first specimen was aged 90 days at room temperature (14 H_v) whereas the second sample was artificially overaged for 210 days at 393 K (8 H_v).

Fig. 2a and b show a bright field (BF) TEM image representing the typical microstructure of the aged Pb–0.08% Ca–x% Sn ($x = 0.6$, 2%) alloys. The micrographs reveal the presence of a very fine and intragranular precipitation of intermetallic phases $Pb_{3-x}Sn_xCa$ for the higher tin content. The average precipitate size measured by image analysis is equal to 2.9 nm (Fig. 2b). The microstructure of the Pb–0.08% Ca–0.6% Sn alloy is sometimes composed of a few alignments of coarse intermetallic precipitates ($\varnothing_m \approx 10$ nm) (Fig. 2a). The presence of these alignments affects the start of the overageing process. In fact, the overageing process proceeds via a discontinuous precipitation

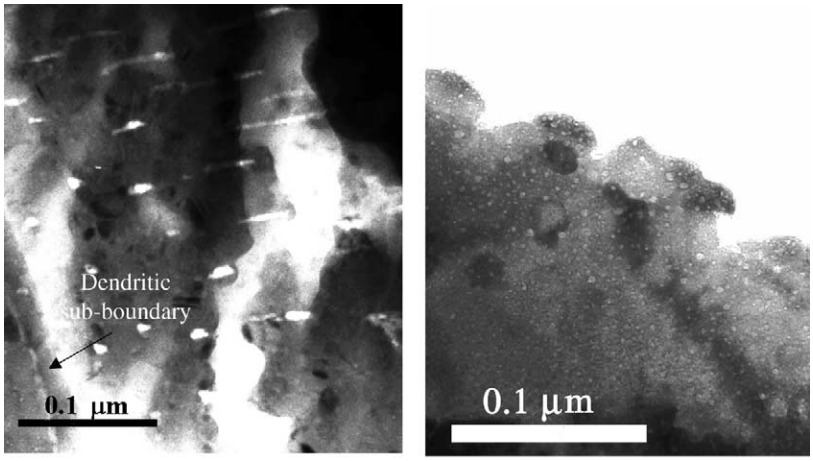

Fig. 2. TEM bright field images of the Pb–0.08% Ca–0.6% Sn (a) and Pb–0.08% Ca–2.0% Sn (b) aged alloys.

[5], which begins on the grain boundaries and on the dendritic sub-boundaries then moves towards the core of the grain. The progression of the reaction front is observed through the alignments of lamellar precipitates [9], which finally gather into lamellae (Fig. 2a):

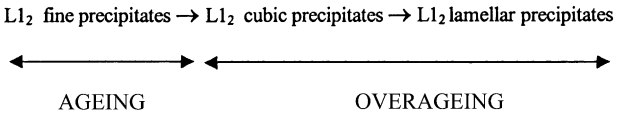

The observations of the overaged alloy microstructure (Fig. 3a and b) indicate the presence of coarse precipitates with a lamellar shape independent of the tin content. Their length and thickness are equal to 3 and 0.2 μm, respectively. EDX analyses of lamellae for overaged alloys show a precipitate tin content increase in accordance with the starting composition of the alloy (Table 2). Moreover, during the overageing, it seems that the precipitate coalescence is accompanied by a rise in tin content. This is well demonstrated by comparison of the precipitate size with the tin precipitate content (see Table 2).

3.2. Corrosion study

3.2.1. Pb–Ca–Sn alloys

The weight loss and the current evolution of the Pb–0.08% Ca–*x*% Sn ($x = 0, 0.6, 2$) alloys corroded for 5 days at 1.5 V in 5 M H_2SO_4 are given in Table 3 and shown in Fig. 4. Three remarks must be made:

- the corrosion of the Pb–Ca alloys ($x = 0$) is not influenced by their metallurgical state;
- for a same Pb–Ca–Sn alloy ($x = 0.6, 2$), the overageing induces a corrosion rate increase;
- whatever the metallurgical state of the alloy, aged or overaged, the higher the tin content, the lower is the weight loss after corrosion in H_2SO_4.

3.2.2. The $L1_2$ phases

The corrosion behaviour at the free potential of the pure phases, in 0.5 M H_2SO_4, i.e. their corrosion potential, is closely related to the tin/lead balance, since the lower the tin content of the intermetallic, the higher its corrosion resistance, as shown in Fig. 5. Pb_3Ca behaves like Pb and is covered by a "protective" layer of $PbSO_4$. On the other

Table 2
$L1_2$ phase composition as a function of the precipitate geometry for Pb–0.08% Ca–0.6% Sn and Pb–0.08% Ca–2.0% Sn overaged alloys

Tin content (wt.%)	Hardness (H_v)	Precipitate morphology[a]	Main geometrical characteristics[b]	Corresponding $L1_2$ phase composition
0.6	7	c	$a \approx 100$ nm	$(Pb_{0.91}Sn_{0.09})_3Ca$
		l	$L \approx 2$ μm, $e \approx 0.2$ μm	$(Pb_{0.83}Sn_{0.17})_3Ca$
2.0	10	c	$a \approx 160$ nm	$(Pb_{0.47}Sn_{0.53})_3Ca$
		l	$L \approx 2$ μm, $e \approx 0.15$ μm	$(Pb_{0.31}Sn_{0.69})_3Ca$

[a] Cubic (c) or lamellar (l).
[b] Edge (a), length (L) and thickness (e).

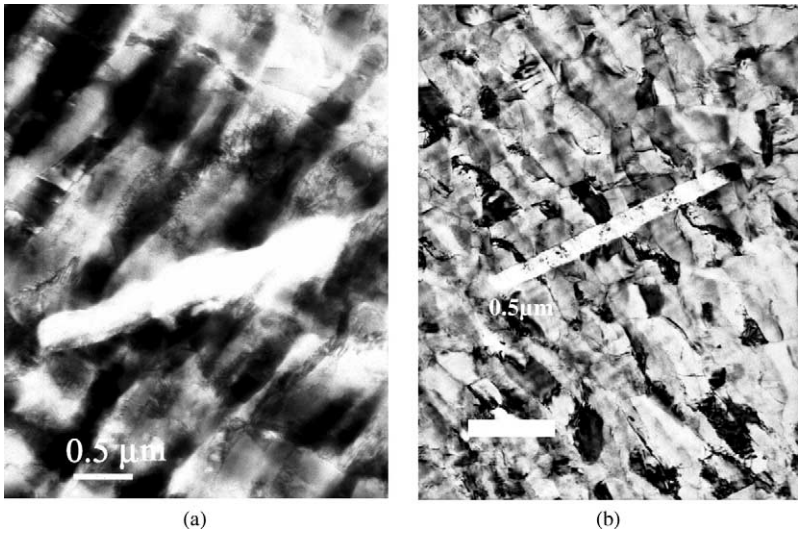

(a) (b)

Fig. 3. TEM bright field images of the Pb–0.08% Ca–0.6% Sn (a) and Pb–0.08% Ca–2.0% Sn (b) overaged alloys.

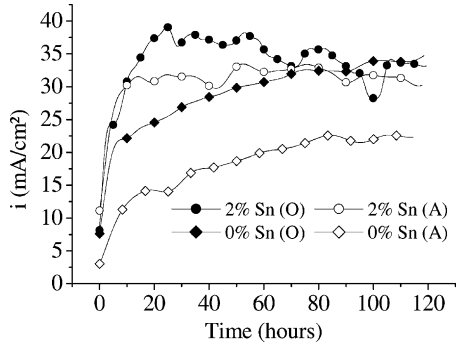

Fig. 4. Current evolution during a potentiostatic oxidation for 5 days at 1.5 V (vs. Hg/Hg_2SO_4) in 5 M H_2SO_4 solution at 323 K. The alloys Pb–0.08% Ca–*x*% Sn were in the aged (A) or overaged (O) metallurgical state.

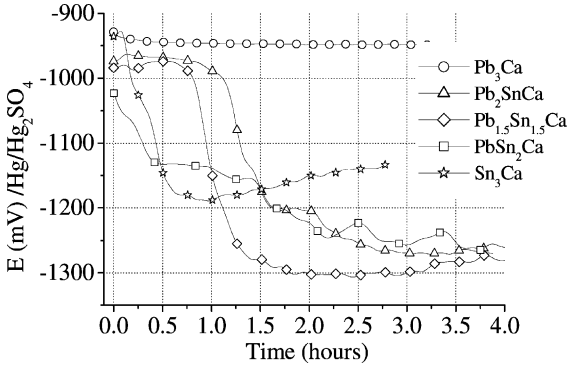

Fig. 5. Corrosion potential of intermetallic compounds in a 0.5 M H_2SO_4 solution.

hand, the binary compound, Sn_3Ca, is never passivated and is totally destroyed at the end of the test. Concerning the pure ternary phases belonging to the $L1_2$ solid solution, Pb_2SnCa, $Pb_{1.5}Sn_{1.5}Ca$ and $PbSn_2Ca$, their corrosion resistance is particularly weak, even if $PbSO_4$ covers the first two alloys at the beginning of the corrosion test, as observed through the plateau of Fig. 5. The potential drop is accompanied by hydrogen evolution.

The three ternary intermetallics undergo a severe attack partly due to a preferential calcium dissolution (Fig. 6). The corrosion layers alternately present metal (free Sn and Pb)

Table 3
Weight loss measurements (mg/cm^2) after a potentiostatic oxidation for 5 days at 1.5 V (vs. Hg/Hg_2SO_4) in 5 M H_2SO_4 solution at 323 K

Alloy	Aged alloys	Overaged alloys
Pb–0.08% Ca	145	148
Pb–0.08% Ca–0.6% Sn	88	160
Pb–0.08% Ca–2% Sn	51	89

The alloys were in the aged and overaged metallurgical states.

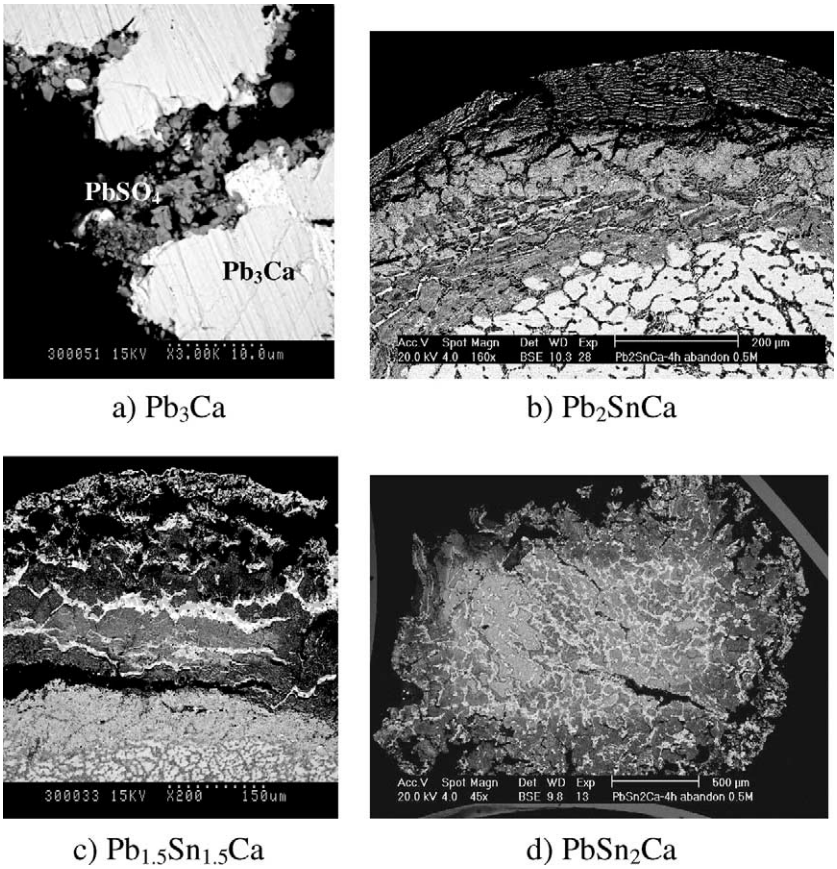

Fig. 6. Metallographic cross-section of four intermetallics after 4 h at the free potential in 0.5 M H_2SO_4 solution.

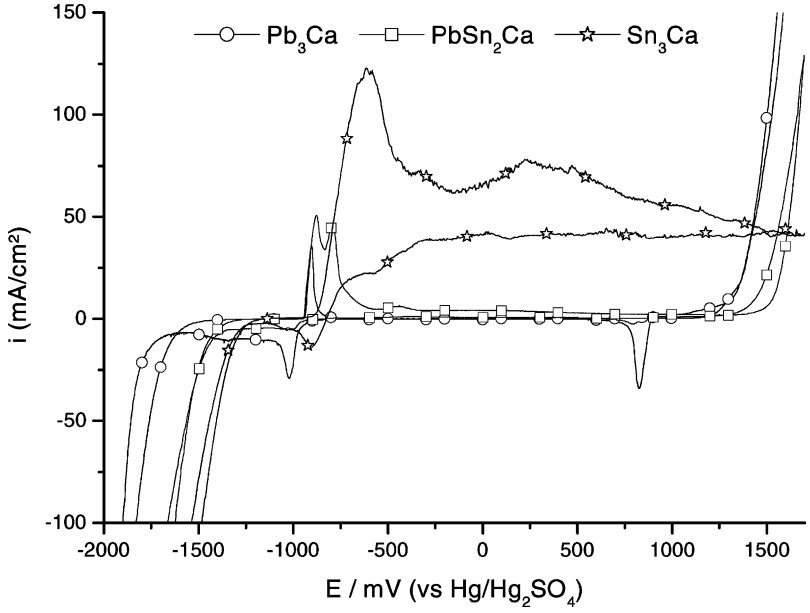

Fig. 7. Characteristic cyclic voltammograms for intermetallic phases in 0.5 M H_2SO_4 solution (sweep rate: 1 mV/s).

and oxide zones. Only the core of the electrode is constituted of the intermetallic, except for $PbSn_2Ca$, which does not contain any stannide after 4 h of testing.

For the four phases coupled with lead and other than Pb_3Ca, which is characterised by a potential similar to that of lead, an anodic behaviour is observed and the corresponding galvanic current strongly depends on the tin level, as in the previous experiment.

Fig. 7 shows the $i = f(E)$ potentiodynamic curve of three pure phases, Pb_3Ca, $PbSn_2Ca$ and Sn_3Ca. The curve of the binary stannide confirms its poor corrosion resistance, since the current density is approximately equal to 40 mA/cm^2 at 1.5 V, a potential for which no hydrogen evolution is observed. The two peaks of the curve of $PbSn_2Ca$ at about −800 and −600 mV correspond to the oxidation of lead and tin, respectively, whereas at higher potential, namely 1.5 V, the anodic current is divided by 10, when it is compared to that of the tin free alloy, Pb_3Ca.

4. Conclusion

Whereas 0.08 wt.% of calcium accelerates the corrosion in the same proportions whatever the metallurgical state of the binary alloy (i.e. aged or overaged), tin has a more subtle effect. Firstly, the greater the amount of this ''active element'', the greater the increase in corrosion resistance for a given metallurgical state of the lead–calcium–tin alloy. Secondly, the overageing is systematically accompanied by an increase of the rate degradation at 1.5 V for a given alloy composition, in conditions of overcharge of lead-acid batteries. The explanation may lie in the level of the tin content of both matrix and precipitate, since the tin content of the $L1_2$ precipitates is raised if its overall concentration in the alloy increases or further to the ageing/overageing transformation. The electrochemical results on the $L1_2$ pure phases show that the higher the tin content of the 3:1 phase the lower the anodic current value at 1.5 V. As the current due to oxygen evolution in the overall current is probably significant, its decrease certainly limits the breakdown of the PbO_2 corrosion layer, and hence the corrosion of the intermetallics. But the proportion of $L1_2$ precipitates in the alloy remains low, of the order of 4% in volume, and their tin enrichment during the ageing/overageing transformation is made at the expense of the tin content of the lead solid solution, which cannot dissolve more than about 1 wt.% in the conditions of thermodynamic equilibrium at room temperature [10–13]. Consequently, it would be mainly the concentration of tin dissolved in the matrix which determines the corrosion resistance. It must be noted that the corrosion rate of the Pb–0.6% Sn alloy is the same as that of the overaged Pb–0.08% Ca–2% Sn alloy, which is certainly at thermodynamic equilibrium. On the other hand, in the ageing conditions, the higher the bulk tin content, the higher the concentration of tin in the oversaturated lead solid solution; so that the corrosion resistance is improved.

The role of tin in the corrosion of the lead calcium tin alloys recalls that of aluminium in magnesium-based alloys, the corrosion of which is clearly correlated to the aluminium content in the α solid solution of magnesium [14].

Finally, contrary to what is mentioned in the literature [4,5,15], the compositions of the $L1_2$ precipitates never reach the limit of the Pb_3Ca–Sn_3Ca solid solution namely Sn_3Ca, although the value of the Sn/Ca ratio in the Pb–0.08% Ca–2% Sn is higher (25) than the required ratio (9). Even if the calcium content of the ternary alloys tested in the

present study is particularly high, it must be acknowledged that intermediate compositions of $L1_2$ plumbo-stannides are able to improve the tensile strength of the alloys and to strongly delay their overageing.

Acknowledgements

This study was financially supported in part by ADEME (Convention No. 9905057). We would like to acknowledge Ted MCRAE (LCSM—University of Nancy) for useful discussions.

References

[1] B. Culpin, A.F. Hollenkamp, D.A.J. Rand, J. Power Sources 38 (1992) 63–74.
[2] D. Pavlov, B. Monakhov, M. Maja, N. Penazzi, J. Electrochem. Soc. 136 (1989) 27–33.
[3] P. Steyer, J. Steinmetz, J.P. Hilger, J. Electrochem. Soc. 145 (1988) 3183–3189.
[4] R.D. Prengaman, J. Power Sources 95 (2001) 223–224.
[5] L. Bouirden, J.P. Hilger, J. Hertz, J. Power Sources 33 (1991) 27–50.
[6] A. Maître, G. Bourguignon, J.M. Fiorani, J. Ghanbaja, J. Steinmetz, Mater. Sci. Eng. A, in press.
[7] J.P. Hilger, J. Power Sources 72 (1998) 184–188.
[8] J.P. Hilger, L. Bouirden, J. Alloys Comp. 236 (1996) 224–228.
[9] L. Muras, P.R. Munroe, S. Blairs, P. Kraulis, Z.W. Chen, J.B. See, J. Power Sources 55 (1995) 119–122.
[10] I. Karkaya, W.T. Thompson, Bull. Alloys Phase Diag. 9 (2) (1987) 144–152.
[11] J.W. Cahn, H.N. Treaftis, Trans. Metall. Soc. AIME 218 (1960) 376–377.
[12] E. Kurzyniec, Z. Wajtaszek, Bulletin de l'Académie Polonaise des Sciences 3A (1951) 131–146.
[13] J. Hertz, C. Fornasieri, J.P. Hilger, M. Notin, J. Power Sources 46 (1993) 299–310.
[14] S. Mathieu, C. Rapin, J. Hazan, P. Steinmetz, Corrosion Sci. 44 (2002) 2737–2756.
[15] R.D. Prengaman, Pb-80, Lead Development Association, London, 1980, p. 34.